

Grey Cast Iron Categorization using Artificial Neural Network

Amany Khaled, Mostafa Rostom A. Atia, Tarek Moussa

Abstract—Grey cast iron (GCI) takes part in a wide range of applications in industry specially automotive one due to its unique properties like castability, machinability, low melting point and low cost as well. It's used in manufacturing engine block, clutches, cylinder head, drum brakes, etc. The cooling rate of GCI affects its microstructure. Consequently, mechanical properties of GCI show strong deviation with the change in the texture of its microstructure. The main challenge with GCI is that surfaces are section sensitive i.e. cutting direction of sample gives different shape of microstructure. Although manual assessment to images gives accurate results, it's susceptible to human error, lack of experience and variation of the operators' performance. Thus, automated image processing has a great contribution in this area. It reduces the amount of time required and increases the accuracy of extracted data. Since artificial neural networks (ANN) are always used in cases that are prone to uncertainty and decision making, software for image processing based on artificial neural networks will be introduced to categorize grey cast iron samples.

Index Terms— grey cast iron, neural networks, image processing, GLCM, co-occurrence matrix, categorization, CLAHE

1 INTRODUCTION

By the late 1780s and early 1800s, within the start of the industrial revolution, several types of materials have become of great importance to the industry and therefore, their study became a real necessity. Grey cast iron (GCI) is an attractive material used in industrial applications due to its some advantageous properties such as good castability, corrosion resistance, machinability, low melting point, low cost, and high damping capacity [1]. The microstructure of GCI is characterized by graphite flakes dispersed into the ferrous matrix. The amount of graphite, its size, morphology and distribution are critical in determining the mechanical behavior of GCI [2]. The widely used method to determine GCI mechanical property based on its microstructure is manual visual inspection by a metallurgical expert. Manual assessment of microstructures is a time consuming task and unbiased decision can't be guaranteed. Thus, automation of GCI image analysis is highly recommended.

2 LITERATURE REVIEW

Cast irons and cast steels make a huge family of ferrous alloys[3]. The commercial production of cast iron in the west did not commence until the 13th century A.D., considerably later [4]. The main advantages of cast irons are their low price and ability to originate products of complex shapes, frequently in a single production step [5]. Therefore, These materials have been selected because they are commonly used by industries, as in, for example, structures of machines, lamination cylinders, main bodies of valves and pumps and gear elements [6].

Graphitic cast irons, including those that contain small amounts of alloying elements, are classified as gray, ductile, and malleable according to graphite shape and method of graphite production [7]. GCI is most commonly used materials out of all other cast irons. What makes cast irons applicable in industry is their microstructure under slow cooling. Graphite flakes found in GCI internal structure reduces the amount of volume reduction in case of slow cooling to zero.

General Motors DAEWOO Auto & Technology Company (GMDAT) has offered the standard EDS-T-7101 to apply microscopic test over GCI microstructures and grade and rate GCI samples. The GMDAT standard presents five classes to characterize the different shapes of graphite particles named from A to E [8]. Details of GMDAT standard pattern classification are illustrated through Fig. 1 and summarized in [9].



Fig. 1 Reference images for the five classes of graphite particles according to standard EDS-T-7101

The morphology and the distribution of graphite grains are the decisive factors in judging the properties of cast iron [10]. Therefore, the assessment of microstructures is an important approach in GCI property analysis. The conventional way of analysis is visual inspection and decision making through a metallurgical expert. This operation can be misleading if the metallurgist was not knowledgeable enough. Therefore, automation of this operation through textural image analysis and artificial neural networks has become of great importance.

Several research areas have adopted statistical image analysis through gray level co-occurrence matrix (GLCM) feature extraction then decision making through (ANN) like in [11] [12] [13].

This research work illustrates the application of using image processing techniques to analyze GCI texture then apply this analysis to an ANN to categorize the grades of GCI. To start

- Eng.Amany Khaled is currently pursuing masters degree program in Mechanical Engineering in Arab academy for science, technology and maritime transport, Egypt, E-mail: amanykhaled@aast.edu
- Assoc. Prof. Mostafa Rostom A. Atia is currently head of mechanical engineering department in Arab academy for science, technology and maritime transport, , Egypt E-mail: mrostrom1@aast.edu
- Dr.Tarek Moussa is the supervisor of materials science laboratory at Ain university- Faculty of Engineering, Egypt. Email: tarekmoussa2001@yahoo.com

grading GCI, there must be a sufficient database of images that fulfils all the desirable grades. Therefore, a microscope was used to capture images. Then image enhancement techniques were applied to improve images quality to undergo textural analysis and feature extraction. At last ANN was used to categorize grades of GCI.

3 EXPERIMENTAL WORK

Following the standard EDS-T-7101, Images need to be captured at a magnification power of $\times 100$. Therefore, an inverted microscope of model Innovatest IN-MM600 was used. Inverted microscopes aren't affected by the changes in the surrounding environment like conventional ones. Therefore, images quality is nearly equal in all captured samples.

3.1 Sample Preparation

Discrimination of cast iron grades is made on unetched surfaces. Eleven specimens of GCI and four specimens of ductile cast iron were chosen such that there's a variety in microstructural shapes and diversity in grades.

Preparations of the metallographic specimens were carried out according to GMDAT standards. Emery paper discs grading from 80 to 1000 grit sizes were used for gradual specimen grinding at 300 rpm. Specimens were cleaned after grinding in methanol in ultrasonic cleaner for 15 minutes. 1 micron alumina powder emulsion in distilled water, embedded in rotating disc cloth, polishing of the specimen surface was performed at 300 rpm. Severe drying was held afterwards to avoid corrosion. Cleaning of specimens was done after drying by methanol in ultrasonic cleaner for additional 15 minutes. Then re-drying was carried out once more. At the end, all samples were put in a well-sealed container over a bed of silica gel to ensure control over humidity in the medium as shown in Fig. 2.



Fig. 2 Samples in silica-gel bed

3.2 Image Capture

Setup shown in Fig. 3 had been used to capture images. A CCD camera is attached directly to the microscopic setup. The main advantage of this setup is that it has stable fixture. The camera is attached to the computer through a 10moons video capture card. Compatible software was used to capture the images and save them in the required format. A sample of captured images is shown in Fig. 4.



Fig. 3 Microscopic setup with CCD camera and attached computer

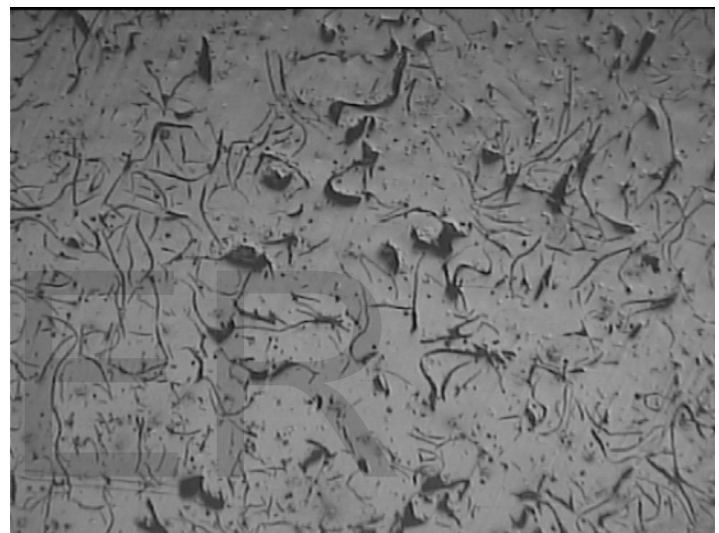


Fig. 4 sample of captured image at magnification $\times 100$

4 IMAGE ENHANCEMENT

Captured images from microscope have a real problem with the variation in contrast and brightness within the same image. This is mainly due to the local imperfections that can be detected on the surface of the sample. Therefore, image enhancement techniques are applied to the captured images to modify them and ensure that they all lie in the same range of contrast and brightness.

Piecewise linear transformation was applied on the image at first. This contrast stretching approach is based on using a sloping function that stretches contrast values of dark areas around the mean of image intensities. As a result, a problem was initiated where borders of the image become darker than the rest of the image as illustrated in Fig. 6-a. To overcome this drawback, logarithmic transformation was used.

Logarithmic transformation expands the dark pixels values concentrated in an area to a wider range while suppressing brighter ones. The more the brightness factor value, the brighter the image get as concluded in Fig. 6-b. However, the value of the brightness factor must be monitored in a manner that doesn't affect the texture under study.

As a final refining step contrast limited adaptive histogram equalization (CLAHE) is used to ensure that values of intensities are all distributed among the histogram of the image.

CLAHE differs from ordinary histogram equalization in the respect that the adaptive method computes several histograms, each corresponding to a distinct section of the image, and uses them to redistribute the lightness values of the image. It is therefore suitable for improving the local contrast of an image. Moreover, the contrast limited adaptive histogram equalization reduces the noise that may be generated over the adaptive technique, giving a more realistic equalized image.

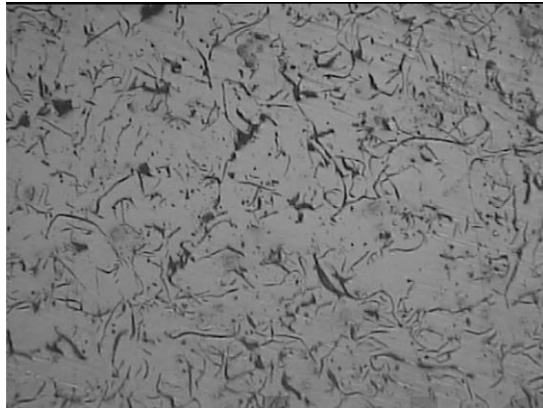


Fig. 5 Original sample image

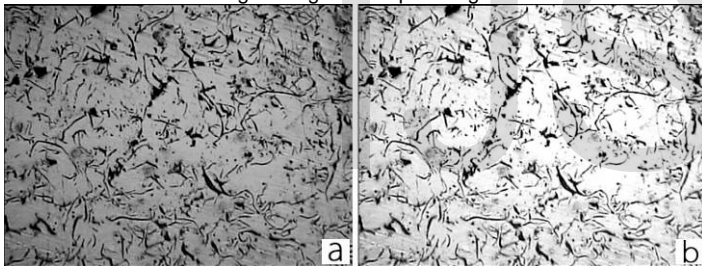


Fig. 6 Image Enhancement Techniques

a) Piecewise transformation b) Logarithmic transformation

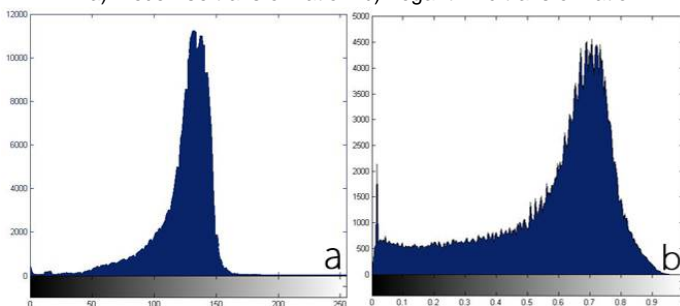


Fig. 7 Image Histogram before and after applying CLAHE

a) Original image b) image after applying CLAHE

5 TEXTURAL ANALYSIS

In 1973, Haralick et al.[14] Defined the texture to be the statistical distribution of tone where tone is the variation of shades of gray color of resolution cells in an image. Two classifications are used to identify the type of texture and therefore, help in analyzing its features. First classification is concerned with the level of homogeneity of the elements that define the

texture itself. The other classification is concerned with texture classification approaches [15].

5.1 Statistical Textural analysis

Statistical texture analysis describes the texture from the perspective of the repetition of certain colors or values through the whole image. The spatial relation and distribution of each tone of color in the introduced texture can be used to define features such as mean, variance, coarseness, etc. These features can then be used to differentiate between textures and define its features.

A very important and widely used set of textural descriptors, in the statistical approach, are obtained from information regarding the relative position of pixels with respect to each other. This information is not carried by individual histograms and is considered as second order statistics, since two joint random variables are considered: the intensities of a reference pixel and a second one, in a different position (an offset $\Delta x, \Delta y$) [16].

5.2 Gray level co-occurrence matrix

Gray level co-occurrence Matrices (GLCM) approach is a statistical one where the relation between each pixel and its neighboring one is considered with respect to their gray levels and probability of occurrence[17]. According to the type of texture and the effect of gray bins (levels), statistical features can be extracted from the GLCM by means of applying some mathematical operations to the probability of occurrence of each level. Haralick et.al [14] introduced a number of features that have been effectively used in several applications afterwards. Gray co-occurrence matrices are calculated as follows

$$M_{co} = \sum_{x=1}^k \sum_{y=1}^k \begin{cases} 1 & \text{if } I(x,y) = i \text{ and } I(x+d_x, y+d_y) = j \\ 0 & \text{otherwise} \end{cases} \quad (1)$$

Where:

- K Image size
- I Image
- d Separating distance
- i reference pixel intensity value
- j Neighbor pixel intensity value

5.3 Feature extraction

According to the type of texture and the effect of gray bins (levels), statistical features can be extracted from the GLCM by means of applying some mathematical operations to the probability of occurrence of each level. Haralick et.al[14] introduced a number of features that have been effectively used in several applications afterwards.

Through different literatures, it has been observed that a number of features were the most common ones used indifferent applications to identify textures. TABLE 1 shows cross mapping between different research papers and the chosen features.

Features used in this research were chosen according to the commonly used features in previous research. TABLE 2 shows

the chosen features and the method of calculation of each. Each feature was calculated through a GLCM of a single separating step between pixels i.e. a window size of 3x3. Moreover, features in all four directions were calculated, and then an average of them was taken to prepare the dataset used in neural network evaluation afterwards.

TABLE 2
CROSS MAPPING OF RESEARCHES AND CHOSEN FEATURES

<i>F</i> <i>paper</i>	1	2	3	4	5	6	7	8	9	10	11	12	13
[18]													
[19]													
[20]													
[21]													
[22]													
[23]													
[24]													
[25]													
[26]													
[27]													
[28]													
[29]													
[30]													
[31]													
[32]													
[33]													
[34]													
[35]													
[36]													

The features discussed by Harralick and others as follows; 1) Energy - 2) Contrast - 3) Correlation - 4) Variance - 5) Homogeneity - 6) Average - 7) Sum variance - 8) Sum entropy - 9) Entropy - 10) Difference variance - 11) Difference entropy - 12) Maximum correlation - 13) dissimilarity

TABLE 1
SELECTED FEATURES EXTRACTED FROM IMAGES

Feature	Mathematical relation
Contrast	$CON = \sum_{i,j} i - j ^2 p(i, j)$
Correlation	$COR = \sum_{i,j} \frac{(i - \mu_x)(j - \mu_y)}{\sigma_x \sigma_y} p(i, j)$
Energy	$ENG = \sum_{i,j} p(i, j)^2$
Entropy	$ENR = \sum_{i,j} p(i, j) \log(p(i, j))$
Homogeneity	$HOM = \sum_{i,j} \frac{1}{1 + (i - j)^2} p(i, j)$
Dissimilarity	$DIS = \sum_{i,j} i - j p(i, j)$

Where :

- i* reference pixel intensity value
- j* Neighbor pixel intensity value
- σ_x standard deviation in x direction
- σ_y standard deviation in y direction
- μ_x mean along x direction
- μ_y mean along y direction

6 NEURAL NETWORKS

Neural networks are usually used in applications where uncertainty of decision exists. They can simulate human's behavior in extracting a certain decision from a set of data supplied earlier for training.

6.1 Dataset preparation

A dataset was prepared to meet the requirements of neural networks training. 370 images of different shapes of microstructures of GCI were all captured and features were extracted from each image separately.

To prepare the analysis of each image, software was developed to meet the requirements of metallurgists in manual assessment. This software, named Gray CIMA: Cast Iron Manual Assessment, was developed using MATLAB. The user chooses the regions of interest and then submits them for calculations. The software, following the GMDAT standard in manual assessment, calculates and displays the percentage of presence of the chosen grade. Fig. 8 shows the graphical user interface of Gray CIMA. Then results can be outputted to an excel sheet.

Validation to this developed software was accomplished by choosing random samples of the processed images and comparing them to manual assessment by expert. Since the software is based on the grid method well known and used by experts, data extracted from it proved to be valid for usage.

7 RESULTS AND DISCUSSION

A number of neural networks were designed and trained to fulfill the required GCI categorization. The two previously discussed networks have shown remarkable results over other networks.

7.1 FFNN - I

Fig. 10 shows a regression of 95% of training and the same for test data. Histogram of errors in Fig. 11 shows high values at the occurrence of a value of 3.79. The main disadvantage of this network is the existence of some error values that exceeded the 5% which will affect the decision significantly in most cases.

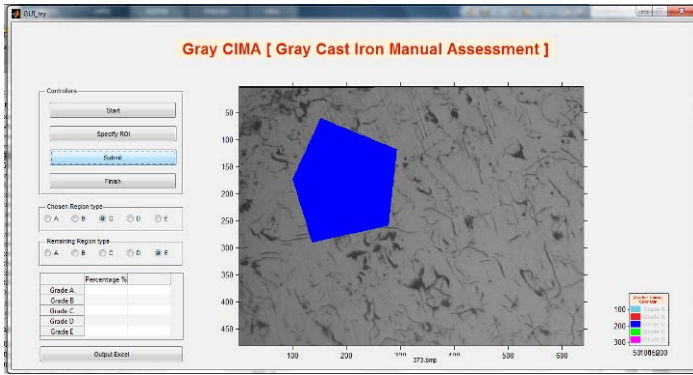


Fig. 8 Gray CIMA user interface

6.2 Neural Network design and training

A number of neural networks were designed and set ready for training. Between varying the training functions, the number of hidden layers and the number of nodes in each layer, remarkable results were overseen through training and testing each network.

Fig. 9 shows the design of feed forward neural network (FFNN) used. This network consists of one hidden layer. Six inputs, which are the features extracted from GLCM, are inputted to the input layer and six outputs which represent the 5 grades of cast iron in addition to ductile cast iron.

Two networks have shown good results. FFNN -I, Training function for the hidden layer was tan sigmoidal function while that of the output layer was pure linear. Hidden layer consisted of 8 neurons. However in FFNN-II, Training function for the both the hidden and output layer is tan sigmoid. Hidden layer consisted of 20 neurons.

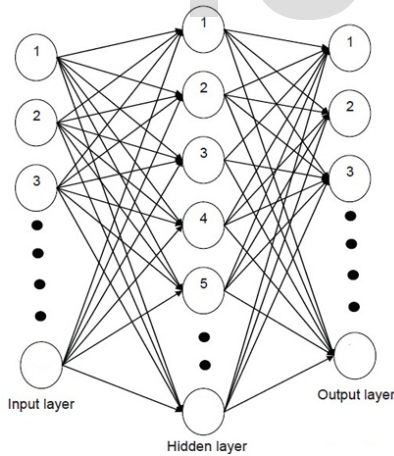


Fig. 9 FFNN schematic representation

Not all records in the dataset were used in training; however, 70% of the whole data were randomly selected to train the network, 15% for testing and 15% for validation.

Machine used for training was of processor Intel Core i7 3rd Gen. of speed 2.0 GHz with turbo boost up to 3.10 GHz and memory 8GB. Operating system was Windows 7 home premium and network training was made with MATLAB 2013a.

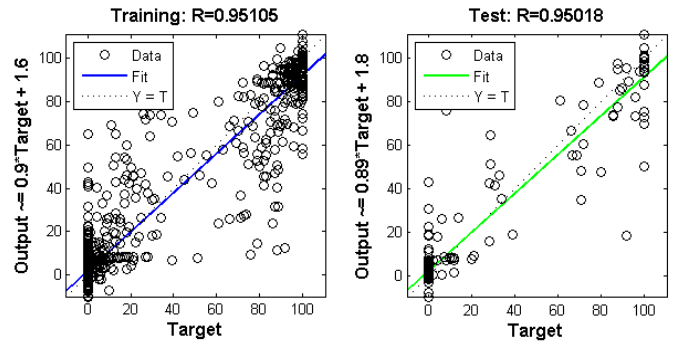


Fig. 10 Regression of training and test results over targets in FFNN-I

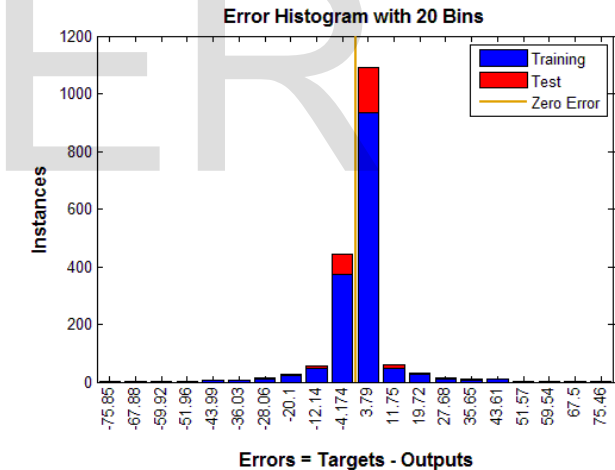


Fig. 11 Errors values histogram for FFNN-I

7.2 FFNN - II

FFNN-II has shown better results than that found in the FFNN-I. For instance, Fig. 12 shows that it has shown better regression around 99.7% in training of samples while in test data, regression became 94.9 %. Errors histogram in Fig. 13 shows better results than that of FFNN where only high repetition of errors was found in values of -3.37 and 3.558 which will not affect the decision in a harmful manner. While other values of errors occurred in very rare cases.

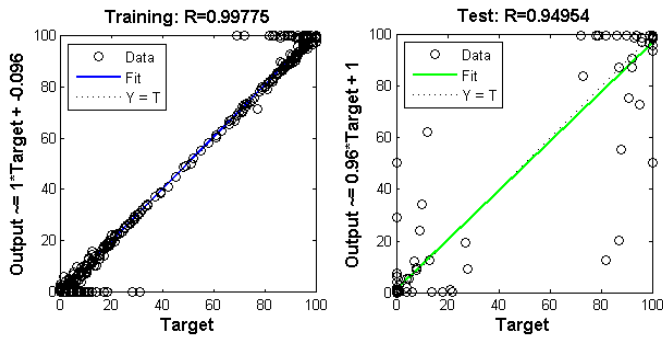


Fig. 12 Regression of training and test results over targets in FFNN-II

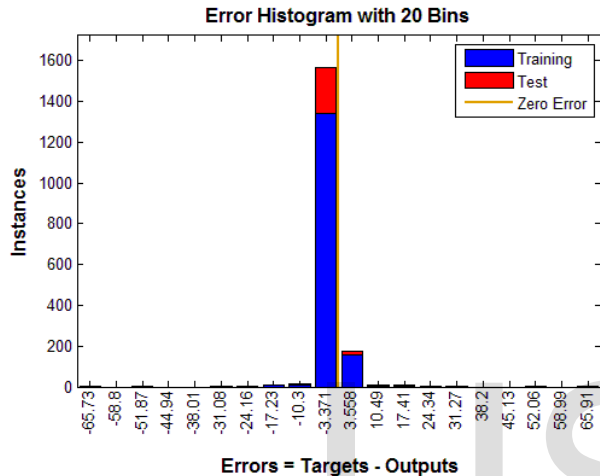


Fig. 13 Errors values histogram for FFNN-II

7.3 Sample of Validation

Random sample images from dataset were used in validation by comparing results of Gray CIMA, the output of the neural network and the results of a commercial software that was associated with the microscope. TABLE 3 shows a sample of result of comparison between results.

TABLE 3
RESULTS COMPARISON

Sample	Results							
	FFNN-I		FFNN-II		Grey CIMA		Commercial Software	
1425	77%D	23%E	89%D	10%E	91%D	9%E	65.8%A	34.2%com.*
1435	48%A	41%C	88%A	12%C	89%A	11%C	65.8%A	34.2%com.
1440	8%C	99%D	11%C	99%D	12%C	88%D	85.7%A	14.3%com.
1450	45%C	57%D	37%C	63%D	37%C	63%D	88%D	12%com.
1479	56%C	45%D	48%C	52%D	48%C	52%D	86.5%C	13.1%com.
D218	100% Not GCI		100% Not GCI		Not GCI		85.5%A	11.5%com.
D215	100% Not GCI		99% Not GCI		Not GCI		83.4%A	13.5%com

*com = combined structure.

It's observed that FFNN-II shows good results compared to that of FFNN-I. The commercial software has shown different results compared to grey CIMA results. Two samples of other structures than grey cast iron were subjected to NN and the

commercial software i.e. samples D218 and D215. All FFNNs have distinguished that those images are not GCI from the beginning. While, on the other side, the commercial software graded the image as flake graphite iron.

FFNN-II has shown highly accurate identification of the grade of the proposed samples, while the commercial software failed in most cases to direct the decision correctly.

Conclusion

In the present research, novel software has been developed for automatic identification and categorization of grey cast iron. The software is based on image processing of microstructure using ANN algorithm. According to GMDAT standard, a number of specimens of different grey cast iron categories were prepared and microstructure structure image were captured and enhanced. These images were assed manually by an expert using software, which was developed by the author. The ANN training sets were prepared using image texture features as input and the manual assessment results as output. After ANN training, it was tested using validation data sets. The tests show that the proposed ANN design, FFNN-II, identified 98% of the submitted samples with a range of error between 3 to 4 %. Moreover, the results were compared with the results of microscope commercial software. The developed software results were more accurate than the commercial one. The software introduced in this research is a step towards atomization of microstructure analysis. In addition, it reduces the analysis time, cost and human fatigue without scarifying accuracy.

References

- [1] Z. Taşlıçukur, G. S. Altuğ, Ş. Polat, Ş. H. Atapek, And E. Türedi, "Characterization Of Microstructure And Fracture Behavior Of Gg20 And Gg25 Cast Iron Materials Used In Valves," 2012.
- [2] S. N. Gurugubelli, "Experimental Investigations On Structure And Mechanical Properties Of Semi Solid Casting Of Gray Cast Iron," *Int. J. Adv. Sci. Res. Technol.*, vol. 3, no. 2, pp. 190-193, 2012.
- [3] I. Rustamov, "Manufacturing Processes," in *Machinery 's Handbook*, 28th ed., 2008, pp. 1266 - 1421.
- [4] D. A. SCOTT, *Metallography and Microstructure of Ancient and Historic Metals*. 1991..
- [5] J. P. Papaa, R. Y. M. Nakamura, V. H. C. de Albuquerque, A. X. Falcão, Joãvaresd, and M. R., "Computer techniques towards the automatic characterization of graphite particles in metallographic images of industrial materials," *Expert Syst. Appl.*, 2012.
- [6] V. H. C. de Albuquerque, P. C. Cortez, A. R. de Alexandria, and J. M. R. S. Tavares, "A New Solution for Automatic Microstructures Analysis from Images Based on a Backpropagation Artificial Neural Network."
- [7] ASM Handbook Committee., "Volume 9; Metallography and Microstructures," in *ASM Handbook*, 9th ed., 1992.

- [8] C. D. T. Mineral, "Automatic Classification of Graphite in Cast Iron," *Microsc. Microanal.*, vol. 11, no. 4, pp. 363–371, 2005.
- [9] H. Jiang, Y. Tan, Z. Zhang, J. Hu, J. Lei, and L. Zeng, "Auto-analysis system for graphite morphology of grey cast iron," *J. Autom. Methods Manag. Chem.*, vol. 25, no. 4, pp. 87–92, Jan. 2003.
- [10] P. Prakash, "Comparative Analysis of Spectral and Spatial Features for Classification of Graphite Grains in Cast Iron," *Sci. Technol.*, vol. 29, no. April, pp. 31–40, 2011.
- [11] S. Jain, "Brain Cancer Classification Using GLCM Based Feature Extraction in Artificial Neural Network," *Methodology*, vol. 4, no. 07, pp. 966–970, 2013.
- [12] S. D. M. Raja and A. Shanmugam, "ANN and SVM Based War Scene Classification Using Invariant Moments and GLCM Features: A Comparative Study," *Mach. Learn.*, vol. 2, no. 6, pp. 869–873, 2012.
- [13] P. K. N. Rode, "Analysis of ms using glcm," *Eng. Technol.*, vol. 1, no. 5, pp. 121–126, 2012.
- [14] R. Haralick, K. Shanmugam, and I. Dinstein, "Textural Features for Image Classification," *IEEE Trans. Syst. Man Cybern. SMC-3*(, vol. 6, pp. 610–621, 1973.
- [15] J. M. Flores, "Texture Characterization and Analysis," *Analysis*, 2010.
- [16] C. Tanchotsrinon, S. Phimoltares, and C. Lursinsap, "An autonomic building detection method based on texture analysis , color segmentation , and neural classification," *Matrix*, pp. 162–167, 2013.
- [17] C. N. Rao, S. S. Sastry, K. Mallika, H. S. Tiong, and K. B. Mahalakshmi, "Co-Occurrence Matrix and Its Statistical Features as an Approach for Identification Of Phase Transitions Of Mesogens," *Int. J. Innov. Res. Sci. Eng. Technol.*, vol. 2, no. 9, pp. 4531–4538, 2013.
- [18] P. K. N. Rode, "Analysis of ms using glcm," *Eng. Technol.*, vol. 1, no. 5, pp. 121–126, 2012.
- [19] D. A. Clausi, "An analysis of co-occurrence texture statistics as a function of grey level quantization," *Design*, vol. 28, no. 1, pp. 45–62, 2002.
- [20] R. O. K. Reddy, "Classifying Similarity and Defect Fabric Textures based on GLCM and Binary Pattern Schemes," *Engineering*, no. November, pp. 25–33, 2013.
- [21] L. B. Mostaço-guidolin, A. C. Ko, F. Wang, B. Xiang, M. Hewko, G. Tian, A. Major, M. Shiomi, and M. G. Sowa, "Collagen morphology and texture analysis: from statistics to classification," pp. 1–10, 2013.
- [22] C. N. Rao, S. S. Sastry, K. Mallika, H. S. Tiong, and K. B. Mahalakshmi, "Co-Occurrence Matrix and Its Statistical Features as an Approach for Identification Of Phase Transitions Of Mesogens," *Eng. Technol.*, vol. 2, no. 9, pp. 4531–4538, 2013.
- [23] R. Quevedo, E. Valencia, J. M. Bastías, and S. Cárdenas, "Description of the enzymatic browning in avocado slice using GLCM image texture," *Change*, 2011.
- [24] D. J. Bermejo, "High definition video quality assessment metric built upon full reference ratios," 2012.
- [25] DHANASHREE GADKARI, "IMAGE QUALITY ANALYSIS USING GLCM," 2004.
- [26] P. Mohanaiah, P. Sathyanarayana, and L. Gurukumar, "Image Texture Feature Extraction Using GLCM Approach," *Int. J.*, vol. 3, no. 5, pp. 1–5, 2013.
- [27] I. Texture and F. Extraction, "MSc THESIS Implementing Texture Feature Extraction Algorithms on FPGA," *Electr. Eng.*, 2009.
- [28] J. M. Flores, "Texture Characterization and Analysis," *Analysis*, 2010.
- [29] R. W. Conners, M. M. Trivedi, and C. A. Harlow, "Segmentation of a High-Resolution Urban Scene Using Texture Operators *," *Image Process.*, pp. 273–310, 1984.
- [30] V. S. Thakare, N. N. Patil, and J. S. Sonawane, "Survey On Image Texture Classification Techniques," *Int. J.*, vol. 4, no. 1, pp. 97–104.
- [31] L. Collini, G. Nicoletto, and R. Kone*, "Microstructure and mechanical properties of pearlitic gray cast iron," *Mater. Sci. Eng. A*, vol. 488, pp. 529–539, 2008.
- [32] A. Gebejes, E. M. Master, and A. Samples, "Texture Characterization based on Grey-Level Co-occurrence Matrix," *Artif. Intell.*, pp. 375–378, 2013.
- [33] A. Rampun, H. StrStrange, and R. Zwiggelaar, "Texture Segmentation Using Different Orientations of GLCM Features," *Image (Rochester, N.Y.)*, 2013.
- [34] G. A. B, M. C. Chandrashekar, and M. Z. Kurian, "Texture Feature Extraction of Video Frames Using GLCM," *Int. J. Eng.*, vol. 4, no. 6, pp. 2718–2721, 2013.
- [35] I. Engineering, "GRAY-LEVEL CO-OCCURRENCE MATRIX CONSIDERING POSSIBLE," *Matrix*, pp. 4206–4212, 2013.
- [36] T. A. Pham, "MSc THESIS Optimization of Texture Feature Extraction Algorithm," *Electr. Eng.*, 2010.